

# Extracting the plastic properties of metal materials from microindentation tests: Experimental comparison of recently published methods

Bruno Guelorget<sup>a)</sup> and Manuel François

*Université de technologie de Troyes, Institut Charles DeLaunay CNRS FRE 2848, 10010 Troyes cedex, France*

Cheng Liu

*National Laboratory for Condensed Matter Physics, Institute of Physics, Beijing 100080, China*

Jian Lu

*Department of Mechanical Engineering, Hong Kong Polytechnic University, Hung Hom Kowloon, Hong Kong*

(Received 10 April 2006; accepted 27 December 2006)

Experimental verifications have been performed on three engineering metals to verify recent methods proposed for extracting stress–strain curves from indentation tests. Their sensitivity to data errors is evaluated. Finally, the factors that might cause the inaccuracy and instability of the proposed methods are discussed, providing information that can be useful for further improving these methods.

## I. INTRODUCTION

Indentation has been widely used for characterizing material properties such as Young's modulus, hardness, or yield stress. Tabor and Stilwell<sup>1–3</sup> proposed a method for determining hardness through spherical and conical indentation, introducing the concept of representative strain.<sup>2</sup> The first authors concerned with determining Young's modulus through indentation were Bulychev et al.<sup>4</sup> Later on, Doerner and Nix<sup>5</sup> proposed a method that was improved by Oliver and Pharr.<sup>6</sup> Consequently, indentation is now a widely used technique for performing measurements on thin films or graded materials (for instance, see Refs. 7–12). Nevertheless, it is still an issue whether the mechanical properties of a material can be obtained from indentation tests.

Several methods have already been published.<sup>13–24</sup> Giannakopoulos et al.<sup>13</sup> have published an energy-based method for extracting plastic properties of bulk materials from instrumented indentation. Introducing a new definition of the representative strain, Dao et al.<sup>14</sup> have proposed another method. Nevertheless, several materials, with different plastic properties, can give the same indentation curve.<sup>25–29</sup> To obtain an unique solution, Bucci et al.<sup>15</sup> and Chollacoop et al.<sup>16</sup> proposed a method using two tips of different apex angles. Cao and Lu proposed three methods. The first one uses spherical indentation.<sup>17</sup> The second one uses sharp indentation with two

different tips.<sup>18</sup> The last one is an energy-based method combined with sharp indentation.<sup>19</sup>

More recently, Ogasawara et al.<sup>21</sup> published a method using only one sharp indentation. Zhao et al.<sup>22</sup> proposed a method to determine not only the plastic properties, but also the elastic ones (Young's modulus) with spherical indentation. These two articles are based on a new definition of the representative strain<sup>30</sup> with a more physical meaning. Beghini et al.<sup>23</sup> published a model of direct and inverse analysis. Their model is compared with real experimental indentations and seems to give good results. It needs several sets of coefficients, which are not given in their article, but can be sent on demand for each class of material. A method based on neural networks has been recently published by Tyulyukovskiy and Huber.<sup>31</sup> This method is supposed to be particularly robust.<sup>32</sup>

This article has been written from the user's point of view. Fundamental questions such as the uniqueness of the solution or the sensitivity to tip defects should be dealt with by the authors of the inverse methods (e.g., see Sec. II. C and Sec. II. E). The aim is to test some of these methods on different specimens to compare the results with the yield stress and strain hardening coefficient determined by another way and to deduce, if possible, if one of these methods is suitable. The compared methods are the three methods of Cao and Lu (spherical indentation,<sup>17</sup> two different tip apex angles indentation,<sup>18</sup> and the energy-based method applied to two different tip apex angles indentation<sup>19</sup>) and Ogasawara et al.'s<sup>21</sup> and Zhao et al.'s<sup>22</sup> methods. These methods have been chosen because they propose quite different strategies: different tip geometries (Berkovich or spherical tip),

<sup>a)</sup>Address all correspondence to this author.

e-mail: bruno.guelorget@utt.fr

DOI: 10.1557/JMR.2007.0213

different numbers of tips (one or two), different definitions of representative strain (Dao's or Ogasawara's), and different bases (curves fitting or energy). Evaluation of neural network-based methods is still to be carried out, but from a user point of view, methods that are straightforward and easier to implement are to be tested first.

## II. SHORT PRESENTATION OF THE METHODS

### A. Cao and Lu's<sup>17</sup> sphere method

Extending Dao et al.'s definition of the representative strain<sup>14</sup> to spherical tip, Cao and Lu have determined a "closed-form expression of indentation load at various indentation depths, which is a function of the representative stresses and reduced Young's modulus." An inverse method is proposed, based on the determination of a power behavior law through the determination of two couples (representative strain and representative stress). Existence, uniqueness, and stability of the solution is addressed.

### B. Zhao et al.'s<sup>22</sup> method

This method is based on the idea that "spherical indentation has the potential for measuring the elastic-plastic properties of a power-law hardening bulk specimen with just one simple test," because several representative strains are involved thanks to the nonautosimilar geometry of the tip. Based on Ogasawara's definition of the representative strain,<sup>30</sup> this method is designed to determine elastic (Young's modulus) and plastic (yield stress and strain hardening coefficient) properties of a bulk material by solving a system of dimensionless equations that were established by means of extensive finite element analysis. For two specific depth-to-tip radius ratios ( $h/R = 0.13$  and  $0.3$ , respectively), representative strains are determined and used as inputs for their inverse method.

### C. Cao and Lu's<sup>18</sup> two Berkovich tips method

First, using dimensional analysis and the finite deformation Taylor-based nonlocal theory of plasticity, a closed-form expression of the size-dependent sharp indentation loading curve is established.<sup>33</sup> Second, based on this expression, an inverse method is proposed, using two couples (representative strain and representative stress) to determine the yield stress and the strain hardening coefficient. This method is supposed to hold even at small penetration depths, where effects of geometrically necessary dislocations cannot be neglected. As in the case of spherical tip, Cao and Lu have systematically investigated existence, uniqueness, and stability of the solution.

### D. Cao and Lu's<sup>19</sup> two Berkovich tips energy-based method

Once again, dimensional analysis and the finite element method are used, but in this method, it is to determine "an energy-based representative strain for conical indentation in elastoplastic materials . . . to establish a one-to-one relationship between the representative stress, the indentation loading curvature and the ratio of reversible work to total work." Once these three data are determined through measurement, two couples (representative strain and representative stress) are deduced and used to determine the yield stress and the strain hardening coefficient. Explorations of influences of frame compliance and tip rounding are carried out, as is a comprehensive evaluation of the stability.

### E. Ogasawara et al.'s<sup>21</sup> method

The specificity of this method is to use only one sharp indenter, and several articles have shown that there is no uniqueness of the solution in such a case.<sup>25–29</sup> This question is successfully addressed by applying this method to several samples (numerical data) supposed to have the same load-displacement curve. The input needed is only the total energy, the maximum depth, and the contact stiffness at maximum depth.

## III. EXPERIMENT

### A. Experimental set-up and measured specimens

The indenter used was a NanoIndenter XP® from MTS Corporation (Eden Prairie, MN). It was equipped with the Continuous Stiffness Measurement option so that penetration depth and load on sample were continuously stored during loading and unloading, and contact stiffness was stored during loading. Indentations were performed on three different materials: semi-hard copper (Young's modulus:  $E = 122$  GPa, yield stress:  $\sigma_y = 182$  MPa, and strain hardening coefficient:  $n = 0.23$ ), stainless steel 316L ( $E = 190$  GPa,  $\sigma_y = 281$  MPa, and  $n = 0.11$ ), and pure aluminum ( $E = 70.4$  GPa,  $\sigma_y \approx 7$ – $20$  MPa, and  $n \approx 0.3$ ). Data for aluminum were found in the literature, and those for copper and steel were measured by the present authors on a uniaxial tensile test machine and were used as reference values in Tables I through IV. Copper and steel specimens were carefully polished with an alumina suspension ( $0.3 \mu\text{m}$ ) to avoid surface hardening. The aluminum specimen is a calibration specimen, and its purity is 99.99%. In case of sharp indentations, two different Berkovich tips were used: a standard one (equivalent to a  $70.3^\circ$  cone) and another one equivalent to a  $80^\circ$  cone. In case of spherical indentations, the radius of the sphere was measured with a scanning electronic microscope and was found equal to  $8.1 \mu\text{m}$ .

TABLE I. Validity range, maximum penetration depth, representative strain, and results of the five compared methods applied to three different specimens. For the definitions of  $E^*$ ,  $\epsilon_{rep}$ ,  $\sigma_{ri}$ , and  $\bar{E}$ , see respective references.

Reference values	Validity range	$h_{max}$ (nm)	$\epsilon_{rep}$ (%)		Aluminum 99.99%	Copper	Stainless steel
				$E$ (GPa)	70.4	122	190
				$\sigma_y$ (MPa)	7–20	182	281
				$n$	0.30	0.23	0.11
				$E/\sigma_y$	3,520–10,057	670	676
Cao sphere [17]	$65 < E/\sigma_y < 700$ see Sec. 5 in Ref. 17	810	7 values from 2.5 to 4.2	$\sigma_y$ (MPa)	24	173	252
Zhao sphere [22]	$2 < \bar{E}/\sigma_r < 3000$ see Sec. 2.B in Ref. 22	2430	2 values 3.7 and 6.7	$n$	0.22	0.30	0.18
				$E/\sigma_r$	710	280	202
				$E$ (GPa)	40	73	108
				$\sigma_y$ (MPa)	112	101	1034
				$n$	0.00	0.40	0.00
Cao 2 Berkovich [18]	$65 < E^*/\sigma_r < 500$ see Sec. 3 in Ref. 18	1800	2 values 1.7 and 3.3	$E^*/\sigma_{r1}$	2244	580	642
				$E^*/\sigma_{r2}$	1526	532	434
				$\sigma_y$ (MPa)	0	145	8
				$n$	0.58	0.14	0.59
Cao energy 2 Berkovich [19]	$25 < E/\sigma_y < 1070$ see Part. IV in Ref. 19	1800	2 values from 1.0 to 1.8 and from 2.4 to 3.2	$\sigma_y$ (MPa)	13	200	19
Ogasawara 1 Berkovich [21]	$100 < \bar{E}/\sigma_r < 3300$ see Sec. 2.2 and Sec. 3.2 in Ref. 21	1800	1 value 1.2	$n$	0.35	0.12	0.61
				$\bar{E}/\sigma_r$	1203	481	330
				$\sigma_y$ (MPa)	1	14	0†
				$n$	0.53	0.56	0.87†

†Eq. (11) of Ref. 21 has no solution, see Sec. V. F.

## B. Methodology

For Zhao et al.’s method, the required maximum depth of penetration of the spherical tip is  $h_{max} = 0.3R$ , i.e., 2.43  $\mu\text{m}$  in our case, with  $R$  as the tip radius. For Cao and Lu’s sphere method,  $h_{max} = 0.1R$ , i.e., 0.81  $\mu\text{m}$ . The maximum depth was then fixed higher than 2.43  $\mu\text{m}$  so that the data of the same test could be used with the two methods. The same procedure was applied with sharp indentation. The actual maximum depths in each case are summarized in Table I.

Cao and Lu’s sphere method consists of extracting a set of 10 couples of representative strain and representative stress ( $\epsilon_r$  and  $\sigma_r$ , respectively) for 10 different depths ( $h_{i/R} = 0.01, 0.02 \dots 0.1$ ), where  $R$  is the radius of the tip. Seven couples among 10 (for  $h_{i/R} = 0.04, 0.05 \dots 0.1$ ) were used for applying the method. This point will be discussed in Sec. IV. C. 2.

## IV. RESULTS

### A. Results

The results are gathered in Table I, where  $E$  is the Young’s modulus,  $\sigma_y$  is the yield stress,  $h_{max}$  is the maximum penetration depth, and  $\epsilon_{rep}$  is the representative strain. For the definitions of the reduced modulus  $E^*$ , the representative strains  $\epsilon_{rep}$  and the representative stresses  $\sigma_{ri}$  and  $\bar{E}$ , please refer to respective references. For each specimen,  $E/\sigma_y$  is given in the line “Reference values” and can be compared with the validity range of two methods given by the authors. For methods whose validity range is not related to  $E/\sigma_y$  (Cao 2 Berkovich, Zhao

sphere, and Ogasawara 1 Berkovich), relevant parameters are given. Stress–strain curves were extracted from data of Table I and are plotted in Figs. 1, 2, and 3, with  $\sigma = E\epsilon$  if  $\epsilon \leq \epsilon_y$  and  $\sigma = K\epsilon^n$  if  $\epsilon \geq \epsilon_y$ . It should be noticed that the representative strains are quite small: the maximum is 6.7%, in the case of Zhao’s method.

In each case, several tests were performed and analyzed. Only one result is reported in Table I, but a stability evaluation is presented in the following section.

### B. Sensitivity to data errors evaluation

In this section, the stability of each method is evaluated by applying them to several tests performed on copper. The two spherical indentation based methods (Sec. IV. B. 1 and Sec. IV. B. 2) were applied to the same tests to compare their results. Idem for the three sharp indentation based methods (Sec. IV. B. 3). The purpose of the present article is not to perform a detailed study on the

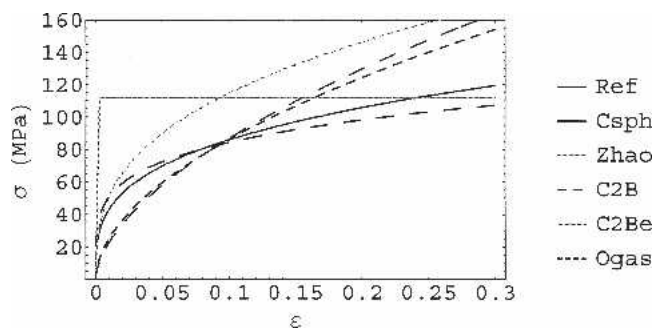


FIG. 1. Stress–strain curves deduced from Table I for aluminum, with reference values  $\sigma_y = 13$  MPa and  $n = 0.3$ .

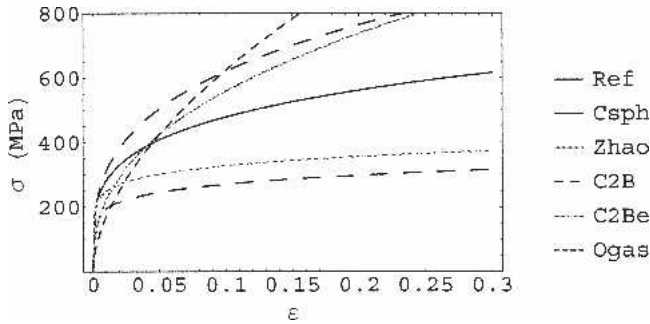


FIG. 2. Stress-strain curves deduced from Table I for copper.

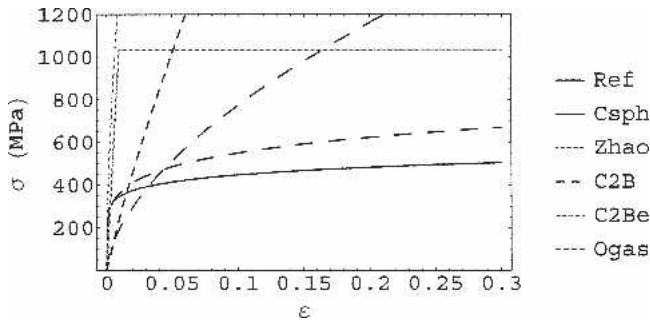


FIG. 3. Stress-strain curves deduced from Table I for stainless steel.

stability of the methods, but only to provide a crude estimation of the dispersions. Stability of such inverse methods applied to two Berkovich tip indentation has already been discussed elsewhere.<sup>34</sup>

### 1. Cao and Lu's sphere method

This method was applied to tests  $S_1$ ,  $S_2$ , and  $S_3$ , plotted on Fig. 4. Even if the maximum depth in these tests is about 3300 nm (Fig. 4), the maximum depth of the used data is 810 nm ( $h/R = 0.1$ ). Results are in Table II. In the present case, this method is stable.

### 2. Zhao et al.'s method

This method was applied to tests  $S_1$ ,  $S_2$ , and  $S_3$ , as in Sec. IV. B. 1. It needs load at two depths (1053 and 2430 nm, i.e.,  $h/R = 0.13$  and  $0.3$ ) and contact stiffness

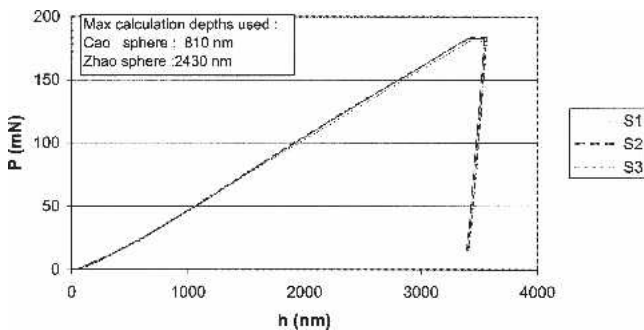


FIG. 4. Three tests on copper used for studying the spherical indentation methods stability. Spherical tip with a 8.1- $\mu$ m radius.

TABLE II. Comparison of three measurements on copper evaluated by Cao and Lu's sphere method.

Tests	$\sigma_y$ (MPa)	$n$
$S_1$	173	0.30
$S_2$	168	0.33
$S_3$	174	0.32
Average	172	0.32

Reference values:  $\sigma_y = 182$  MPa,  $n = 0.23$ .

at one depth (2430 nm, i.e.,  $h/R = 0.3$ ). Thanks to the Continuous Stiffness Measurement option, stiffness was continuously stored, therefore it is an available data even if unloading did not occur at 2430 nm but at 3300 nm (Fig. 4). This method is based on the research of the minimum of a several variables function,  $f(E, \sigma_r, \text{ and } n)$ , to deduce  $E$ ,  $\sigma_r$ , and  $n$ . Thus, before running this method, the inputs of the minimum and maximum limits for each variable  $E$ ,  $\sigma_r$ , and  $n$  are required. When running on large ranges for each variable (for instance  $1 \text{ GPa} < E < 1000 \text{ GPa}$ ,  $1 \text{ MPa} < \sigma_r < 500 \text{ MPa}$ ,  $0.0 < n < 0.6$ ), it appeared that there were many local minima. More restricted ranges have to be introduced. Thus, when applied to experimental data, this method is very sensitive to the limit values given to each variable and would need to implement advanced minimization algorithms to be more reliable. Results are gathered in Table III.

### 3. Sharp indentation-based methods

The two sharp indentation methods of Cao and Lu need two tests made with two tips of different apex angles.

These methods were applied to the three tests whose curves are plotted in Fig. 5 (tip apex angle equivalent to a  $70.3^\circ$  cone), each time associated with the same test with a tip equivalent to a  $80^\circ$  cone ( $B_1 + B_4$ ,  $B_2 + B_4$ , and  $B_3 + B_4$ ). The method by Ogasawara et al. was applied to

TABLE III. Results given by Zhao's method applied to copper specimens.

Test number	Imposed limits for numerical solving						Identified values		
	$\sigma_r$ (MPa)		$n$		$E$ (GPa)		$E$ (GPa)	$\sigma_y$ (MPa)	$n$
	Min	Max	Min	Max	Min	Max			
$S_1$	1	5000	0.0	0.6	1	1000	18	5000	0.00
	300	800	0.0	0.5	50	200	70	249	0.22
$S_2$	1	5000	0.0	0.6	1	1000	18	5000	0.00
	300	800	0.0	0.5	50	200	50	73	0.50
$S_3$	300	800	0.0	0.5	20	200	76	44	0.50
	300	800	0.0	0.4	20	200	63	524	0.00
$S_3$	1	5000	0.0	0.6	1	1000	18	5000	0.00
	300	800	0.0	0.5	50	200	50	75	0.50

Reference values:  $E = 122$  GPa,  $\sigma_y = 182$  MPa,  $n = 0.23$ .

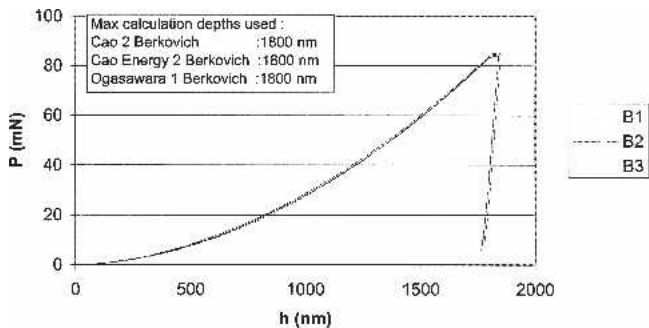


FIG. 5. Three tests on copper used for studying the sharp indentation methods stability. Berkovich tip with an angle equivalent to a  $70.3^\circ$  cone.

the same three tests in Fig. 5 ( $B_1$ ,  $B_2$ , and  $B_3$ ), and results are presented in Table IV.

## V. Discussion

### A. General considerations

First, it is worth noting that the chosen materials do not always fall into the validity range of the methods given by their authors. These methods can give reasonably good results, even outside of their validity ranges, or give poor results even inside.

Two parameters were to be fitted (three in case of Zhao et al.'s method): the yield stress,  $\sigma_y$ , and the strain hardening exponent,  $n$ . Discussions below are based on Table I because even a small error on  $n$  may cause a large scattering of the curves (Figs. 1, 2, and 3).

Generally speaking, numerical inverse methods rely, explicitly or not, on several assumptions: perfect tip, homogeneity of the sample, no size effect, etc.

The shape quality of the spherical tip used was good and was checked by scanning electron microscopy imaging. Tip defects could only be very local differences between an ideal  $8.1\text{-}\mu\text{m}$  radius sphere and the actual one. In case of spherical indentation, maximum penetration depths were 810 and 2430 nm in the present study. The smallest depth used was 324 nm (Cao and Lu's sphere method, with  $h/R = 0.04$ ). Such a depth may be considered as large enough with regard to any tip defect.

TABLE IV. Comparison of the three sharp indentation based methods applied to the same tests.

Cao 2 Berk			Cao 2 Berk energy			Ogasawara		
Tests	$\sigma_y$ (MPa)	$n$	Tests	$\sigma_y$ (MPa)	$n$	Tests	$\sigma_y$ (MPa)	$n$
$B_1 + B_4$	125	0.18	$B_1 + B_4$	168	0.18	$B_1$	0	0.88
$B_2 + B_4$	145	0.14	$B_2 + B_4$	159	0.19	$B_2$	14	0.56
$B_3 + B_4$	96	0.25	$B_3 + B_4$	168	0.18	$B_3$	5	0.63
Average	122	0.19		165	0.18		6	0.69

Reference values:  $\sigma_y = 182$  MPa,  $n = 0.23$ .

In case of sharp indentations, depths used were always greater than 1000 nm. At such depths, the tip defect (estimated at around 20 nm with the Loubet et al.'s method<sup>35,36</sup>) is negligible.

Concerning the homogeneity of specimens, the copper and steel samples were supposed to be homogeneous, and the polishing was very slight, with an alumina suspension, to avoid any strain hardening. The aluminum sample is a monocrystal reference sample, thus, its homogeneity is guaranteed.

Influences of size effect are to be further investigated. If size effect has significant influence, it should be mostly in case of the Cao and Lu sphere method because the smallest depths were used there. This discussion takes place in the following section (Sec. V. C. 2).

None of these methods is perfect. The representative strain never exceeds a few percent (see Table I), thus these methods are much more adapted to catch the yield stress (characteristic of the elastic-to-plastic transition) than the strain hardening coefficient (characteristic of the far plastic range). This is the first source of instability. Moreover, the validation of the representative strain concept is still the subject of active research.<sup>24,37,38</sup>

### B. Cao and Lu's sphere method

Even if aluminum lies outside the validity domain of this method, the results presented in Table I are good ( $\sigma_y = 24$  MPa and  $n = 0.22$ , instead of  $\sigma_y = 7\text{--}20$  MPa and  $n = 0.30$ ). Copper and stainless steel are inside the domain and the results are rather good ( $\sigma_y = 173$  MPa and  $n = 0.30$ , instead of  $\sigma_y = 182$  MPa and  $n = 0.23$  for copper;  $\sigma_y = 252$  MPa and  $n = 0.18$ , instead of  $\sigma_y = 281$  MPa and  $n = 0.11$  for steel). The stability is quite satisfactory.

Strictly speaking, this method consists first in extracting a set of 10 couples of representative strain and representative stress ( $\epsilon_r$  and  $\sigma_r$ ) for 10 different depths ( $h_i/R = 0.01, 0.02 \dots 0.1$ , where  $R$  is the radius of the tip), and second in choosing two couples among this set (flowchart 1 of Ref. 17 proposes those corresponding to  $h_i/R = 0.01$  and  $0.06$ ).

It has been found from experimental results that it is better to use more than two points, but up to seven for depths  $h_i/R = 0.04, 0.05 \dots 0.1$ , and not to take into account depths corresponding to  $h_i/R = 0.01, 0.02$ , and  $0.03$  (i.e., depths equal to 81, 162, and 243 nm). At such depths, small defects may not be negligible anymore. These defects could be in the homogeneity of the specimen (small surface hardening because of polishing...), in the homogeneity of the tip shape, because of size effect, or from roughness. Actually, this was particularly sensitive for copper, and not at all for aluminum. Therefore, this phenomenon is probably from defects at the extreme surface and may be attributed to slight polishing effects, to the residual roughness (roughness after polishing), or

to slight size effect. The method was applied with seven points for all three samples. Trials were made with four, five, and six points, and results were stable.

### C. Zhao et al.'s method

All materials are in the validity range. It seems to be very difficult for this method to give reliable values for  $n = 0.00$  instead of 0.30 for aluminum, 0.40 instead of 0.23 for copper, and 0.00 instead of 0.11 for steel. For  $\sigma_y$ , the result is better for copper (101 MPa instead of 182) but very poor for other specimens (112 MPa instead of 7–20 for aluminum, 1034 MPa instead of 281 for steel). This method provides Young's modulus as well, but never very well. This method gave very good results on numerical examples.<sup>22</sup> The main problem with this method, when applied to experimental data, is the stability (Table III). It is highly sensitive to the limits given to the software before numerical solving, and this tends to show that there are many local minima in the optimized function. An advanced optimization algorithm should give much better results.

Another point is the intrinsically higher instability when fitting the same experimental (always a little bit noisy) data to obtain three variables (Zhao et al.'s method) than to obtain only two.

### D. Cao and Lu's two Berkovich tips method

The main disadvantage to this method is its narrow validity domain, as mentioned in Ref. 22. None of the materials is in the validity domain as given by the authors. It is a pity because they are widely used in the industry. The results for aluminum (0 MPa instead of 7–20 and 0.58 instead of 0.30) and steel (8 MPa instead of 281 and 0.59 instead of 0.11) are unrealistic, and are a little bit better for copper (145 MPa instead of 182 and 0.14 instead of 0.23), but it is quite stable. Although in Ref. 18, it has been shown for stainless steel that a good estimation can be made on the flow stress using a standard Berkovich indenter, the present research shows that it is still very difficult to determine the yield strength and strain hardening exponent accurately by applying micro-indentation to a small scale and the method in Ref. 18.

The principle of Cao and Lu's sharp indentation methods is basically to fit a  $Ke^n$  curve through two points. Even if it is theoretically possible, this approach is likely to give inaccurate results because two points are not enough for a good and stable fitting of experimental data, especially with nonlinear functions such as a power law function.

### E. Cao and Lu's two Berkovich tips energy-based method

Aluminum does not lie in the validity domain, but it is the material for which the identification procedure gives

the best results (13 MPa instead of 7–20 and 0.35 instead of 0.30). For copper, only  $\sigma_y$  can be determined with a reasonable accuracy (200 MPa instead of 182), but the identified values in the case of steel are completely wrong (19 MPa instead of 281 and 0.61 instead of 0.11). This method has some advantages: its large validity domain and its very good stability.

As mentioned in the preceding section, fitting a curve through only two experimental points is likely to give inaccurate results, even if it is theoretically possible, because of the unavoidable measurement noise.

### F. Ogasawara et al.'s method

All of the materials are in the validity domain, but this method gave poor results when applied to experimental data, whereas it gave good results on numerical examples.<sup>21</sup> It is worth noting that for the steel specimen, Eq. (11) of Ref. 21 has no solution. This equation is supposed to give the strain hardening exponent  $n$ . This fact is quite surprising. Maybe that problem could be attributed to a mistype in a published parameter. (An erratum has been published about the representative strain definition,<sup>39,40</sup> but to our knowledge, nothing about the method itself. Consequently, this erratum has no influence on the present results.) The value of  $n$ , which minimizes (in absolute value) the left-hand side of the equation, was taken as an approximate solution and is reported in Table I.

This method is energy based and uses a meaningful definition of the representative strain, therefore, it should be possible to highly improve its results.

## VI. CONCLUSION

Several recently published methods to deduce stress–strain curve from indentation tests have been compared with experimental measurements. It should be emphasized that these methods are more adapted to catch the yield stress than the strain hardening coefficient because materials are tested at the very beginning of plastic range where the strain hardening is still not very sensitive. Two of the methods (Cao and Lu's two Berkovich and Ogasawara et al.'s methods) gave poor results. Among the three remaining, Cao and Lu's sphere method seems to be the more reliable. It should be noted that the present work is a first attempt to experimentally check the methods on specific materials. The use of other materials could have given different results. Nevertheless, Zhao et al.'s method is highly sensitive to the limits given before numerical solving, thus, its use requires much care and advanced optimization algorithm, even if it is based on a definition of the representative strain with a more physical meaning. The energy-based dual sharp indenters method appears to be stable, but taking the advantage of

the spherical indentation into consideration, further extension of the energy-based representative strain to spherical indentation is important and necessary: an energy-based method with spherical indentation remains to be developed, and a new definitions of representative strain (as those of Ogasawara et al.<sup>30</sup> or Cao and Huber<sup>38</sup>) are worth trying into such a scheme.

Finally, most of the time, the published inverse methods do not take into account several points that can have a strong influence on the results; for instance, what about the tip rounding effect,<sup>41,42</sup> the influence of the friction between the tip and the material,<sup>42–45</sup> the uniqueness of the solution,<sup>25–29</sup> the influence of the experimental noise,<sup>34</sup> a possible orthogonality defect between the sample and the tip axe, effects of the unavoidable roughness,<sup>46,47</sup> and size effect?<sup>48–50</sup> Further investigations are still needed to reach a really reliable method validated on experimental data.

## ACKNOWLEDGMENT

The authors gratefully acknowledge the referees for their helpful comments.

## REFERENCES

1. D. Tabor: A simple theory of static and dynamic hardness, in *Proc. R. Soc.* **92**, 247 (1948).
2. D. Tabor: *Hardness of Metals* (Cambridge University Press, Cambridge, UK, 1951).
3. N.A. Stilwell and D. Tabor: Elastic recovery of conical indentations, in *Proc. Phys. Soc.* **LXXVIII**, 169 (1961).
4. S.I. Bulychev, V.P. Alekhin, M.K. Shorshorov, A.P. Ternovskii, and G.D. Shnyrev: Determining Young's modulus from the indenter penetration diagram. *Zovod. Lab.* **41**, 1137 (1975).
5. M.F. Doerner and W.D. Nix: A method for interpreting the data from depth-sensing indentation instruments. *J. Mater. Res.* **1**, 601 (1986).
6. W.C. Oliver and G.M. Pharr: An improved technique for determining hardness and elastic modulus using load and displacement sensing indentation experiments. *J. Mater. Res.* **7**, 1564 (1992).
7. K.W. Lee, Y.W. Chung, C.Y. Chan, I. Bello, S.T. Lee, A. Karimi, J. Patscheider, M.P. Delplancke-Ogletree, D. Yang, B. Boyce, and T. Buchheit: An international round-robin experiment to evaluate the consistency of nanoindentation hardness measurements of thin films. *Surf. Coat. Technol.* **168**, 57 (2003).
8. T. Chudoba, N. Schwarzer, V. Linss, and F. Richter: Determination of mechanical properties of graded coatings using nanoindentation. *Thin Solid Films* **469–470**, 239 (2005).
9. S. Chowdhury, M.T. Laugier, and I.Z. Rahman: Measurement of the mechanical properties of carbon nitride thin films from the nanoindentation loading curve. *Diam. Relat. Mater.* **13**, 1543 (2004).
10. L.Y. Huang, J. Lu, and K.W. Xu: The nano-scratch behaviour of different diamond-like carbon-film substrate. *Appl. Phys.* **37**, 2135 (2004).
11. V. Nelea, H. Pelletier, P. Mille, and D. Muller: High-energy ion beam implantation of hydroxyapatite thin films grown on TiN and ZrO<sub>2</sub> inter-layers pulsed laser deposition. *Thin Solid Films* **453–454**, 208 (2004).
12. T. Roland, D. Reirant, K. Lu, and J. Lu: Fatigue life improvement through surface nanostructuring of stainless steel by means of residual mechanical attrition treatment. *Scripta Mater.* **54**, 1949 (2006).
13. A.E. Giannakopoulos and S. Suresh: Determination of elastoplastic properties by instrumented sharp indentation. *Scripta Mater.* **40**, 1191 (1999).
14. M. Dao, N. Chollacoop, K.J. Van Vliet, T.A. Venkatesh, and S. Suresh: Computational modeling of the forward and reverse problems in instrumented sharp indentation. *Acta Mater.* **49**, 3899 (2001).
15. J.L. Bucaille, S. Stauss, E. Felder, and J. Michler: Determination of plastic properties of metals by instrumented indentation using different sharp indenters. *Acta Mater.* **51**, 1663 (2003).
16. N. Chollacoop, M. Dao, and S. Suresh: Depth-sensing instrumented indentation with dual sharp indenters. *Acta Mater.* **51**, 3713 (2003).
17. Y.P. Cao and J. Lu: A new method to extract the plastic properties of metal materials from an instrumented spherical indentation loading curve. *Acta Mater.* **52**, 4023 (2004).
18. Y.P. Cao and J. Lu: Size dependent sharp indentation. II. A reverse algorithm to identify plastic properties of metallic materials. *J. Mech. Phys. Solids* **53**, 49 (2005).
19. Y.P. Cao, X.Q. Qian, J. Lu, and Z.H. Yao: An energy-based method to extract plastic properties of metal materials from conical indentation tests. *J. Mater. Res.* **20**, 1194 (2005).
20. N. Chollacoop and U. Ramamurty: Experimental assessment of the representative strains in instrumented sharp indentation. *Scripta Mater.* **53**, 247 (2005).
21. N. Ogasawara, N. Chiba, and X. Chen: Measuring the plastic properties of bulk materials by single indentation test. *Scripta Mater.* **54**, 65 (2006).
22. M. Zhao, N. Ogasawara, N. Chiba, and X. Chen: A new approach to measure the elastic-plastic properties of bulk materials using spherical indentation. *Acta Mater.* **54**, 23 (2006).
23. M. Beghini, L. Bertini, and V. Fontanari: Evaluation of the stress-strain curve of metallic materials by spherical indentation. *Int. J. Solids Struct.* **43**, 2441 (2006).
24. H. Pelletier: Predictive model to estimate the stress-strain curves of bulk metals using nanoindentation. *Tribol. Int.* **39**, 593 (2006).
25. Y.T. Cheng and C.M. Cheng: Can stress-strain relationships be obtained from indentation curves using conical and pyramidal indenters? *J. Mater. Res.* **14**, 3493 (1999).
26. K.K. Tho, S. Swaddiwudhipong, Z.S. Liu, K. Zeng, and J. Hua: Uniqueness of reverse analysis from conical indentation tests. *J. Mater. Res.* **19**, 2498 (2004).
27. J. Alkorta, J.M. Martín-Esnoala, and J. Gil Sevillano: Absence of one-to-one correspondence between elastoplastic properties and sharp-indentation load-penetration data. *J. Mater. Res.* **20**, 432 (2005).
28. J. Alkorta, J.M. Martín-Esnoala, and J. Gil Sevillano: Erratum: "Absence of one-to-one correspondence between elastoplastic properties and sharp-indentation load-penetration data." *J. Mater. Res.* **20**, 1369 (2005).
29. O. Casals and J. Alcalá: The duality in mechanical property extraction from Vickers and Berkovich instrumented indentation experiments. *Acta Mater.* **53**, 3545 (2005).
30. N. Ogasawara, N. Chiba, and X. Chen: Representative strain of indentation analysis. *J. Mater. Res.* **20**, 2225 (2005).
31. E. Tyulyukovskiy and N. Huber: Identification of viscoplastic material parameters from spherical indentation data: Part I. Neural networks. *J. Mater. Res.* **21**, 664 (2006).

32. D. Klötzer, C. Ullner, E. Tyulyukovskiy, and N. Huber: Identification of viscoplastic material parameters from spherical indentation data: Part II. Experimental validation of the method. *J. Mater. Res.* **21**, 677 (2006).
33. Y.P. Cao and J. Lu: Size dependent sharp indentation. I. A closed-form expression of the indentation loading curve. *J. Mech. Phys. Solids* **53**, 33 (2005).
34. Y.P. Cao and J. Lu: Depth-sensing instrumented indentation with dual sharp indenters: Stability analysis and corresponding regularization schemes. *Acta Mater.* **52**, 1143 (2004).
35. J-L. Loubet, M. Bauer, A. Tonck, S. Bec, and B. Gauthier-Manuel: *Nanoindentation with a Surface Force Apparatus* (Kluwer Academic Publishers, Dordrecht, The Netherlands, 1993), pp 429 and 447.
36. G. Hochstetter, A. Jimenez, and J-L. Loubet: Strain-rate effects on hardness of glassy polymers in the nanoscale range. Comparison between quasi-static and continuous stiffness measurements. *J. Macromol. Sci.-Phys.* **B38**, 681 (1999).
37. N. Chollacoop and U. Ramamurty: Robustness of algorithms for extracting plastic properties from the instrumented sharp indentation data. *Mater. Sci. Eng., A* **423**, 41 (2006).
38. Y.P. Cao and N. Huber: A further investigation on the definition of the representative strain in conical indentation. *J. Mater. Res.* **21**, 1810 (2006).
39. N. Ogasawara, N. Chiba, and X. Chen: Erratum: "Representative strain of indentation analysis" [*J. Mater. Res.* 20, 2225 (2005)] and "Limit analysis-based approach to determine the material plastic properties with conical indentation". *J. Mater. Res.* **21**, 2699 (2006). [*J. Mater. Res.* 21, 947 (2006)].
40. H. Pelletier, J. Krier, A. Cornet, and P. Mille: Limits of using bilinear stress-strain curve for finite element modeling of nanoindentation response on bulk materials. *Thin Solid Films* **379**, 147 (2000).
41. J.M. Antunes, L.F. Menezes, and J.V. Fernandes: Three-dimensional numerical simulation of Vickers indentation tests. *Int. J. Solids Struct.* **43**, 784 (2006).
42. B. Taljat and G.M. Pharr: Development of pile-up during spherical indentation of elastic-plastic solids. *Int. J. Solids Struct.* **41**, 3891 (2004).
43. M. Mata and J. Alcalá: The role of friction on sharp indentation. *J. Mech. Phys. Solids* **52**, 145 (2004).
44. H. Habbab, B.G. Mellor, and S. Syngellakis: Post-yield characterisation of metals with significant pile-up through spherical indentations. *Acta Mater.* **54**, 1965 (2006).
45. D.L. Joslin and W.C. Oliver: A new method for analyzing data from continuous depth-sensing microindentation tests. *J. Mater. Res.* **5**, 123 (1990).
46. M.S. Bobji and S.K. Biswas: Deconvolution of hardness data obtained from nanoindentation of rough surfaces. *J. Mater. Res.* **14**, 2259 (1999).
47. M.R. Begley and J.W. Hutchinson: The mechanics of size-dependent indentation. *J. Mech. Phys. Solids* **46**, 2049 (1998).
48. W.D. Nix and H. Gao: Indentation size effects in crystalline materials: A law for strain gradient plasticity. *J. Mech. Phys. Solids* **46**, 411 (1998).
49. I. Manika and J. Maniks: Size effects in micro- and nanoscale indentation. *Acta Mater.* **54**, 2049 (2006).